Case Studies in Structural Engineering 2 (2014) 41–51

Contents lists available at ScienceDirect

Case Studies in Structural Engineering

journal homepage: www.elsevier.com/locate/csse

Strain test and stress intensity assessment of a CPR1000 Nuclear Power Plant pressurizer during pre-delivery hydrostatic test

Lin Lei *, Xu Decheng, Yu Min, Xue Fei, Jiang Jiawang, Zhang Guodong, Zhao Wensheng

Suzhou Nuclear Power Research Institute, Suzhou, China

ARTICLE INFO

Article history:
Available online 12 October 2014

Keywords:
Pressurizer
Strain test
Pre-delivery hydrostatic test
Stress intensity
Fatigue usage factor

ABSTRACT

Strain gages are applied to get the strain and stress of a CPR1000 Nuclear Power Plant (NPP) pressurizer during the pre-delivery hydrostatic test. The measured strain curves are discussed to find the deformation features of the cylinder. The stresses of cylindrical base metal, longitudinal welds and girth welds are calculated and compared with the theoretical values. The stresses in girth welds and upper head nozzle welds show non-uniformity at these areas. The possible reasons are discussed for this phenomenon. The stress intensity is calculated and evaluated according to the allowable limit. The fatigue usage factor is evaluated by considering the effect of internal pressure rise-and-fall cycle to pressurizer's total fatigue life. The evaluated results show that the hydrostatic test has little effect on the integrity or fatigue life of the pressurizer. This test provides the basic deformation data of the pressurizer, which plays an important role in the ageing assessment and management during operation.

Introduction

Pressurizer is one of the most important equipment installed in Nuclear Island (NI) in Nuclear Power Plant. It takes the role of pressure controlling of the primary loop. Generally, pressurizer is a cylindrical vessel with hemispherical heads. In theory, the stress distribution within the pressurizer surface is uniform, if the pressure in the vessel is uniform. The two popular theories for cylindrical vessel stress analysis are thin-walled cylinder theory and thick-walled cylinder theory [1–4].

The effect of the hydrostatic test is the inspection of strength and airtightness [5,6] of the pressurizer. In a hydrostatic test, the internal pressure increases from zero to pressurizer's design, operating and test level. So this process is useful to evaluate the integrity of the pressurizer. For the intensity assessment of pressurizer, hydrostatic test is only one step of the assessment. Stress analysis is also important for the intensity assessment. Stress analysis is used very widely for researches. For example, stress analysis under internal pressure has been performed a lot for nozzle-to-pipe [7,8] and nozzle-to-sphere [9,10] connections.

Leak inspection and geometry inspection are usual methods to evaluate the integrity of pressurizer during the hydrostatic test. However, these inspections cannot get the direct data about the stress condition. Researchers performed some tests and simulations to evaluate the effect of hydrostatic. Rao et al. discussed the failure cases relevant to the pressurizer hydrostatic test [11]. Bhuyan analyzed the retardation effect of a steel gas cylinder with prostatic retest load [12]. Stress and stability analysis has been performed for thick laminated pressure vessels and shells [13–17].

* Corresponding author at: Suzhou Nuclear Power Research Institute, 215004 Suzhou, China. Tel.: +86 512 65353761; fax: +86 512 68701561.
E-mail address: linlei@cgnpc.com.cn (L. Lin).

http://dx.doi.org/10.1016/j.csse.2014.09.002
2214-3998/

Nomenclature

σ_z	longitudinal stress
σ_θ	hoop stress
σ_r	radial stress
P_i	internal pressure
P_o	external pressure
t	cylinder thickness
D	cylinder diameter
r	radius
ra_{thin}	the ratio of measured stress to the thin-walled theoretic stress value
ra_{thick}	the ratio of measured stress to the thick-walled theoretic stress value
R_i	inner diameter of the cylinder
R_o	outside diameter of the cylinder
$\sigma_{\theta i}$	hoop stress of the cylinder inner surface
$\sigma_{\theta o}$	hoop stress of the cylinder external surface
σ_{zi}	longitudinal stress of the cylinder inner surface
σ_{zo}	longitudinal stress of the cylinder external surface
K	the radius ratio of spherical head, $K = R_o/R_i$
E	the modulus of elasticity
μ	the Poisson's ratio
α	coefficients of linear expansion
ε_1	hoop strain
ε_2	longitudinal strain
σ_1, σ_2	the principal stresses
σ_{max}	the maximum and minimum principal stresses
$\varepsilon_{0^\circ}^{min}$, ε_{45° and ε_{90°	strain at 0°, 45°and 90°direction
P_m	general primary membrane stress intensity;
S_y	material yield strength;
S_m	material allowable basic stress intensity value;
S_u	material tensile strength;
U_i	the fatigue usage factor;
N_A	the allowable cycle number at specified stress amplitude.

Most researchers focus on the finite element analysis method to get the stress or strain distribution of the vessel [18,19]. However, there are uncertainties during the fabrication process which will lead to differences between the design and actual structural stress. For the high radiation dose at operating period, it is even impossible to get the real stress distribution data by the conventional strain test method. Thereof, it is important to get such basic data before the pressurizer is installed in NI. This paper concerns the actual strain and deformation features, stress distribution properties and the stress intensity during the hydrostatic test. Biaxial and triaxial strain gauges are used to get the actual strain variation data. The elastic theory is used to obtain the stress values from the strain data. Then comparison of longitudinal and hoop stresses at different locations of the pressurizer is performed. Stress and fatigue assessments are performed according to the RCC-M [20] requirements.

Analysis model

When the cylinder thickness is much smaller than its diameter, it is called thin-walled cylinder. Under uniform internal pressure, any point in the cross section of the cylinder shows two-direction stress state, which can be described as follows:

$$\sigma_z = \frac{P_i D}{4t} \tag{1}$$

$$\sigma_\theta = \frac{P_i D}{2t} \tag{2}$$

According to the thick-walled cylinder theory, under uniform internal pressure, any point in the cross section of the cylinder shows three-direction stress state, and shows stress gradient along thickness. The radial stress cannot be ignored. For a thick-walled cylinder under internal and external pressure, the stress in the cross section with radius r can be described as follows:

$$\sigma_\theta = \frac{P_i}{K^2 - 1}\left(1 + \frac{R_o^2}{r^2}\right) \tag{3}$$

$$\sigma_r = \frac{P_i}{K^2 - 1}\left(1 - \frac{R_o^2}{r^2}\right) \tag{4}$$

$$\sigma_z = \frac{P_i}{K^2 - 1} \tag{5}$$

At the internal surface, $r = R_i$, the stresses are:

$$\sigma_\theta = P_i\frac{K^2 + 1}{K^2 - 1}, \quad \sigma_r = -P_i, \quad \sigma_z = \frac{P_i}{K^2 - 1} \tag{6}$$

At the external surface, $r = R_o$, the stresses are:

$$\sigma_\theta = \frac{2P_i}{K^2 - 1}, \quad \sigma_r = 0, \quad \sigma_z = \frac{P_i}{K^2 - 1} \tag{7}$$

Thus, according to the thick-walled theory, the hoop and longitudinal stress ratios are as follow:

$$\frac{\sigma_{\theta i}}{\sigma_{\theta o}} = \frac{K^2 + 1}{2}, \quad \frac{\sigma_{zi}}{\sigma_{zo}} = 1 \tag{8}$$

For a point in the cross section with radius r, the stresses of spherical head are described as follows [21]:

$$\sigma_r = \frac{P_i}{K^3 - 1}\left(1 - \frac{R_o^3}{r^3}\right) \tag{9}$$

$$\sigma_\theta = \sigma_z = \frac{P_i}{K^3 - 1}\left(1 + \frac{R_o^3}{2r^3}\right) \tag{10}$$

From Eqs. (9) and (10), it shows that the radial stress is compressive along the thickness. At the internal surface, the σ_r is $-P_i$. At the external surface, it is zero. Hoop stress equals to longitudinal stress and is a tensile stress. At the internal surface, they are:

$$\sigma_{\theta i} = \sigma_z = \frac{p}{K^3 - 1}\left(1 + 0.5K^3\right) \tag{11}$$

At the external surface, the hoop stress and longitudinal stress are:

$$\sigma_{\theta o} = \sigma_z = \frac{1.5p}{K^3 - 1} \tag{12}$$

The ratio of internal hoop stress to external hoop stress is:

$$\frac{\sigma_{\theta i}}{\sigma_{\theta o}} = \frac{1 + 0.5K^3}{1.5} \tag{13}$$

The external surface of the pressurizer cylinder presents plane strain state during the hydrostatic test. The principal stresses can be calculated applying generalized Hooke's Law. The principal stress of cylinder can be calculated by Eq. (14) as follows:

$$\begin{cases} \sigma_1 = \frac{E}{1-\mu^2}(\varepsilon_1 + \mu\varepsilon_2) \\ \sigma_2 = \frac{E}{1-\mu^2}(\varepsilon_2 + \mu\varepsilon_1) \end{cases} \tag{14}$$

For discontinuities in lower and upper head, the principal stress is calculated by Eq. (15),

$$\sigma_{\substack{\max \\ \min}} = \frac{E}{2}\left[\frac{\varepsilon_{0^\circ} + \varepsilon_{90^\circ}}{1 - \mu} \pm \frac{1}{(1 + \mu)}\sqrt{(\varepsilon_{0^\circ} - \varepsilon_{90^\circ})^2 + [2\varepsilon_{45^\circ} - (\varepsilon_{0^\circ} + \varepsilon_{90^\circ})]^2}\right] \tag{15}$$

Test procedure and relevant records

Pressurizer description and the theoretical stress values

The pressurizer discussed in this paper is used in a CPR1000 NPP which is manufactured according to the RCC-M standard. The total height of the pressurizer is 12.84 m and is placed horizontally during the hydrostatic test. Its design pressure is 17.13 MPa, and the operating pressure is 15.4 MPa. The material of cylinder, upper and lower head is 16MND5, and austenitic stainless steel is overlaid on it. 16MND5 is C–Mn–Ni–Mo steel, and the material properties at 20 °C are as follows,

Table 1
Design and actual geometry parameters of the pressurizer.

	Design values (mm)		Measured values (mm)	
	Inner diameter	Thickness	Inner diameter	Thickness
Cylinder	2134 ± 7	⩾113	2134	⩾120.4
Girth weld between upper head and the cylinder	2134 ± 7	⩾108	2134	⩾112.1
Longitudinal weld in cylinder	2134 ± 7	⩾108	2134	⩾120.4
Upper head	1093 ± 5	⩾66	1093	⩾93.2
Lower head	1083 ± 8	⩾83	1083	⩾93

Table 2
Theoretical external surface stress values of the pressurizer at 23.6 MPa.

	Thin-walled theory		Thick-walled theory	
	σ_z (MPa)	σ_θ (MPa)	σ_z (MPa)	σ_θ (MPa)
Cylinder	105.80	211.61	100.21	200.43
Girth weld between upper head and the cylinder	112.32	224.63	106.71	213.42
Longitudinal weld in cylinder	104.57	209.15	98.99	197.98

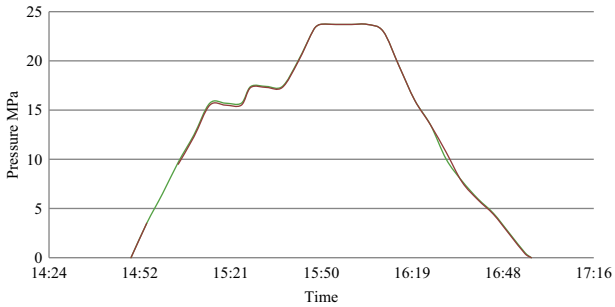

Fig. 1. Pressure record curves during the hydrostatic test.

E = 204 GPa, μ = 0.3, $\alpha = 11.22 \times 10^{-6}/°C$, S_y = 345 MPa, S_m = 184 MPa, and S_u = 552 MPa. The design geometry parameters of the pressurizer and measured values after fabrication are listed in Table. 1. The factor K is then calculated as follows:

(1) For cylindrical and longitudinal weld in the cylinder: K = 1.113;
(2) For girth weld in the cylinder: K = 1.105;
(3) For the upper head: K = 1.171;
(4) For the lower head: K = 1.172.

According to Eqs. (1)–(5), the theoretical stresses of the pressurizer at the highest hydrostatic test pressure based on the measured geometries are calculated and shown in Table 2.

Hydrostatic test procedure and parameter records

The highest hydrostatic test pressure is 23.6 MPa, and the temperature of external surface during the hydrostatic test is maintained at 36 °C. During the hydrostatic test, the internal pressure increases from 0 to 23.6 MPa, and maintained for at least 10 min at 15.4 MPa and 17.13 MPa. The measured internal pressure variation curve is shown in Fig. 1 and the test holds for about 2 h. During the hydrostatic test, the measurement points of circumference changes are at location A, B and C, where B is at the middle of the cylinder, C is near the upper head and with a 4200 mm distance from B, A is near the lower head and with a 4000 mm distance from B. The circumference measurement layout and test results are shown in Fig. 2a and Fig. 2b, which show that the circumferential deformation decreases from lower vessel to upper vessel.

3. Strain test method

The KFG-1-120-D16-11 biaxial rectangular strain gauges are applied at the cylinder. The KFG-1-120-D17-11 triaxial strain gauges are mounted at structure discontinuities in upper and lower heads. The DH5927 data acquisition system is

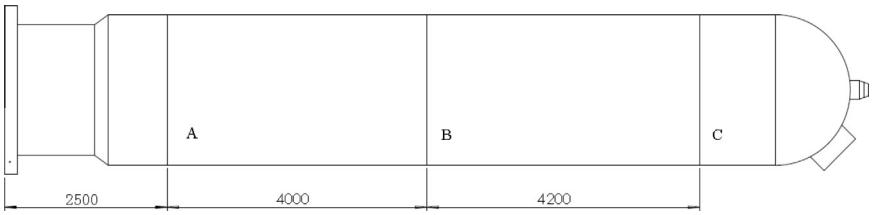

Fig. 2a. Circumference measuring point layout.

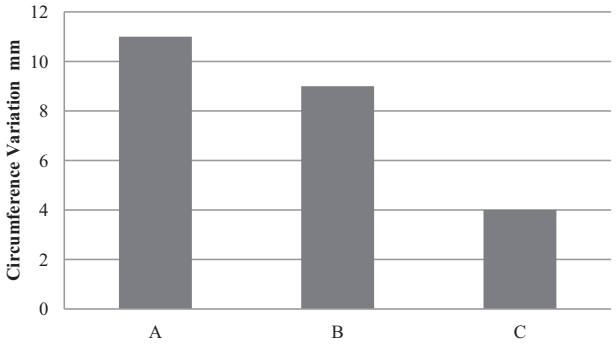

Fig. 2b. Circumference variation after and before the hydrostatic test.

applied to get the strain variation data. The measuring points' layouts are shown in Figs. 3–5. Along the longitudinal direction, there are three measurement points in the pressurizer base metal, which are named as T1, T2 and T3. And there are three measurement points in the longitudinal welds along the longitudinal direction, which are named as Z1, Z3 and Z5. Points Z2, Z4 and Z6 are defined at the symmetric location of Z1, Z3 and Z5, and located at the base metal surface. Four measurement points are defined in the girth welds, which are named as H1–H4. The location of H1 and H2 is symmetric, and so do H3 and H4. At the circle where T2 locates, four measurement points around T2 are arranged, which are named as T4, T5, T6 and T7. The angle between T4 and T5 is 15°. Two symmetric measurement points X1 and X2 are defined in the weld of surge line nozzle in lower head. One measurement point named T8 is defined in the base metal of upper head. Seven measure points are defined in upper head nozzle welds. SP1 and SP2 are symmetrically located in the spray nozzle weld. SR1 and SR2 are symmetrically located in the manhole weld. SA1 and SA2 are symmetrically located in the valve nozzle weld. SA3 is defined in another valve nozzle weld.

The strain gauges are mounted at the pressurizer after the pressurizer is filled with water and heated up at 36 °C. The strain test starts to record data while the hydrostatic test begins and continues record until the pressure decreases to zero. The purpose is to get the stress values caused only by the internal pressure at three pressure stages, operating pressure, design pressure and testing pressure.

Results and discussion

Strain measurement data review

Satisfied strain data are obtained during the hydrostatic test. Strain variation curves are shown in Figs. 6–9. Seen from Fig. 6, it indicates the uniformity of strain distribution at different locations of cylindrical base metal external surface. The longitudinal strain values of points T1–T4 are almost equal, and the hoop strain values of these points vary a little.

Strain curves of longitudinal welds are shown in Fig. 7, which indicates differences at different locations in the welds. And the strain values decrease from the lower part of the cylinder to the upper part, which have the same trend as the circumference deformation.

Fig. 8 shows two symmetric points' strain curves. Point Z1 is located in the longitudinal weld and Z2 in the base metal. From Fig. 8, the strain curves of these two points show good consistence. And the same trend is for strain curves of point Z3 and Z4.

Fig. 9 shows the strain curves of girth welds. The strain values decrease from the lower part of the cylinder to the upper part which indicates the same trend as the circumference deformation. It is also noted that even in the symmetric location of a same girth weld, the strain values differ a lot. However, strain values of point H3 matches well with point H4.

The strain curves of upper head and lower head surface or welds are not provided because the strain gauges direction is different.

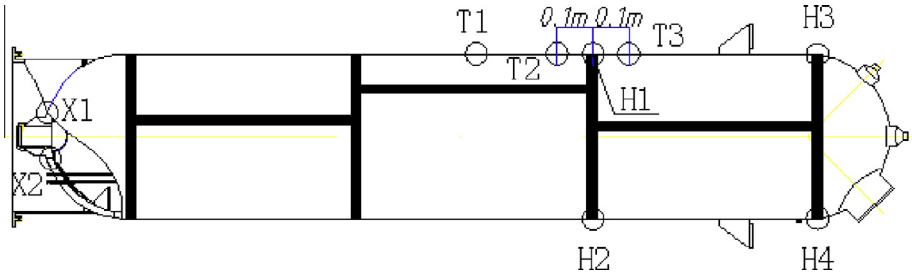

Fig. 3. Strain gages layout for cylindrical circle welds and surge line weld.

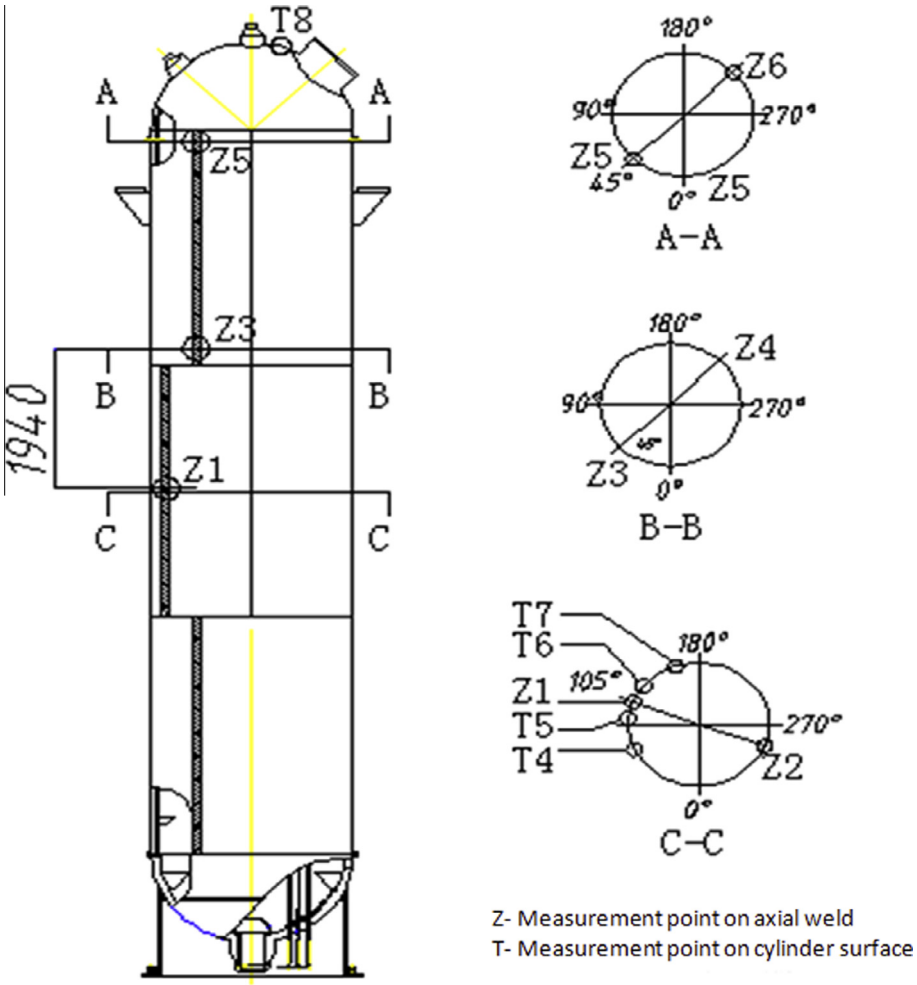

Fig. 4. Strain gages layout for cylindrical and longitudinal weld.

Stress calculation and comparison

The stresses of each point at internal pressure of 23.6 MPa are calculated using Eqs. (14) and (15) as Tables 4–7. The measured values are compared with theoretical values for base metal surface of cylinder and the ratios of test value to theoretical value are listed in the table. From Table 3, the longitudinal and hoop stress of cylinder welds is more consistent with the thick-walled theory. Stress values in girth welds are smaller than the theoretical values, and stress values in longitudinal welds are in good accordance with the theoretical values.

Table 4 shows the stress results of the base metal in the pressurizer cylinder. Seen for the figure, there is a very good consistence between the measured and theoretical stress values. However, stress values of point T5 are much lower than the

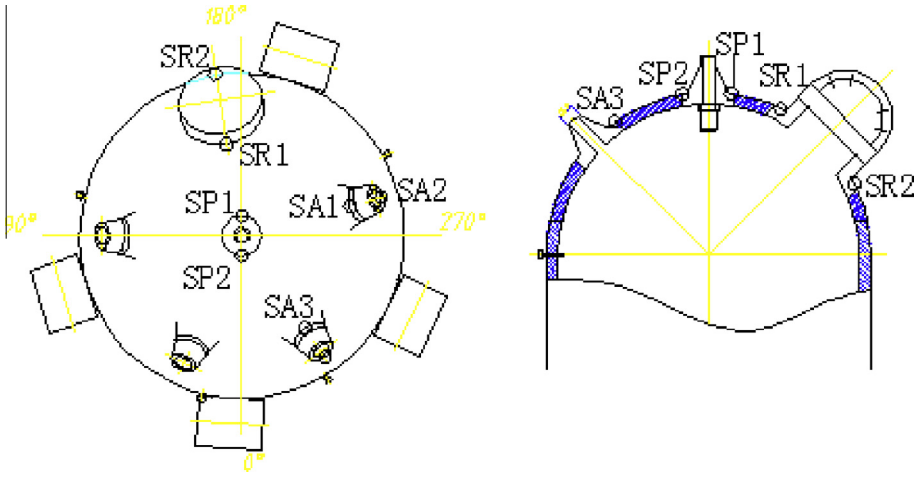

Fig. 5. Strain gages layout for upper and lower head.

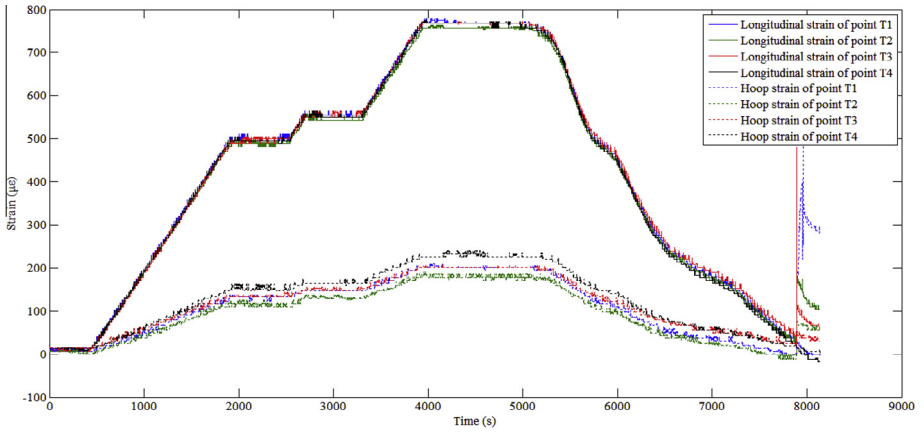

Fig. 6. Strain curves of the base metal in cylinder's external surface.

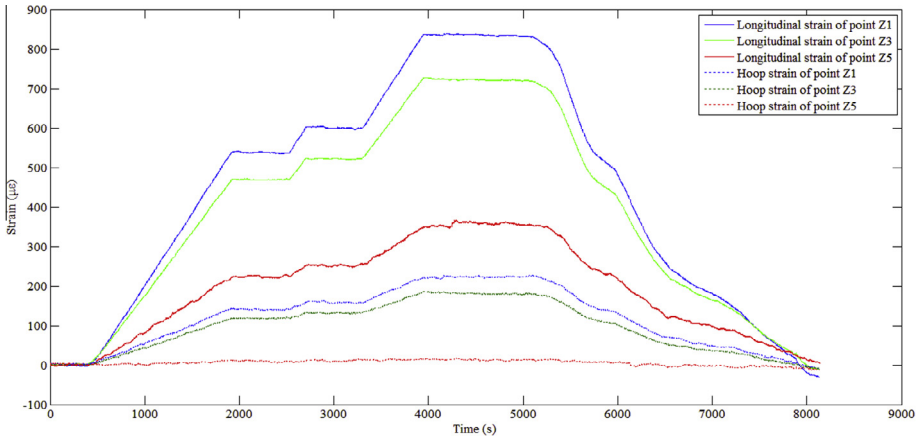

Fig. 7. Strain curves of the longitudinal weld in cylinder's external surface.

theoretical values. T5 is near the longitudinal weld in middle of cylinder. The stress values of point Z1 are in good accordance with that of cylindrical base metal, which indicates that the residual stress in the centerline of longitudinal welds is near zero. Then from the stress values of T5, it is possible that compressive residual stress exists at both sides of longitudinal welds and the compressive residual stress values decrease with the distance from the centerline of the longitudinal weld.

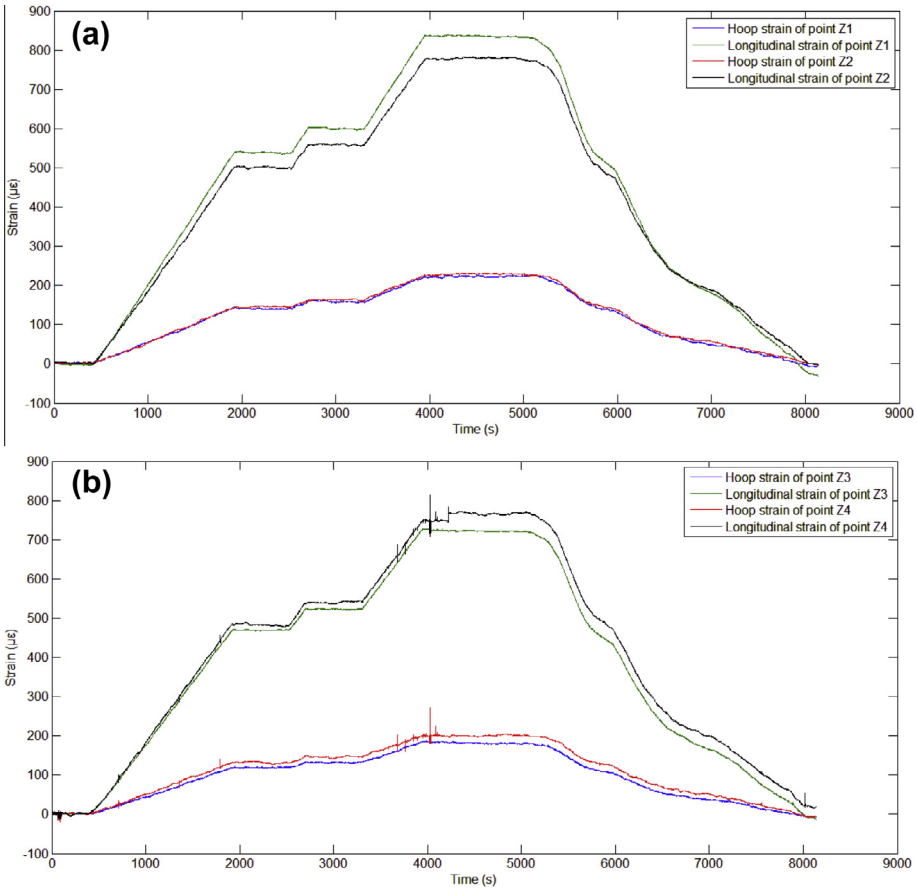

Fig. 8. Strain curves of the longitudinal welds and these symmetry base metal surfaces in the cylinder.

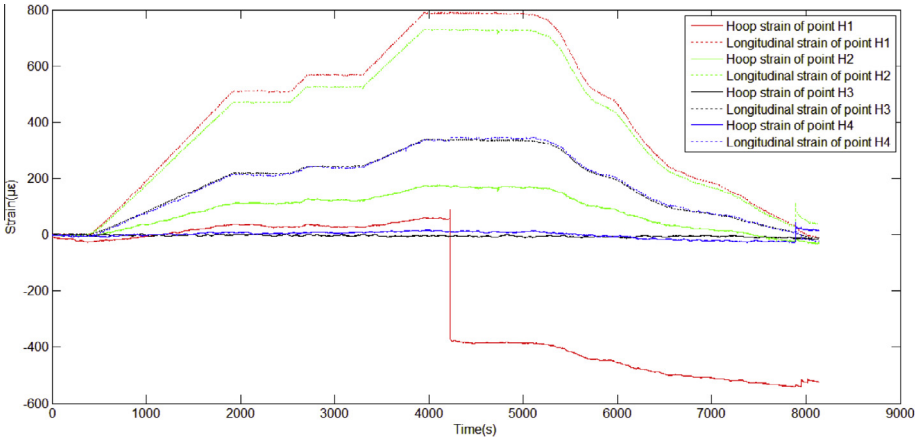

Fig. 9. Strain curves of the girth welds in cylindrical external surface (Strain gauges of point H2 failed during test).

The principal stresses in upper head welds shown in Table 5 indicate the asymmetric distribution. Stress values ratio for two symmetrical points in the same weld differs from 36% to 95%. This shows a possibility that the weld thickness varies along the weld circumference. Another possibility is relevant to the residual stress in the welds.

Table 6 indicates that the stress values in upper head base metal do not follow the spherical stress theory, which reflects the asymmetrical thickness of the upper head. Points H3, H4 and Z5 are in the geometrical discontinuity areas and the stress distribution is complicated. The theoretical stress values for these locations are not calculated. The principal stresses for two points in the surge line nozzle in Table 7 show a good agreement, which illustrates a good geometric symmetry.

Table 3
Stress results in the pressurizer cylinder welds (MPa).

Location	Results comparison	Girth weld of cylinder				Longitudinal weld of cylinder		
Point ID		H1	H2	H3	H4	Z1	Z3	Z5
Longitudinal stress	Test results	88.74	73.06	21.95	26.1	106.9	90.8	28.07
	Thin-walled theory	112.32	112.32	–	–	104.57	104.57	–
	ra_{thin} (%)	79.01	65.05			102.23	86.83	
	Thick-walled theory	106.71	106.71	–	–	98.99	98.99	–
	ra_{thick} (%)	83.16	68.47			107.99	91.73	
Hoop stress	Test results	175.7	182.9	75.81	78.64	203.3	175.8	83.89
	Thin-walled theory	224.63	224.63	–	–	209.15	209.15	–
	ra_{thin} (%)	78.22	81.42			97.20	84.05	
	Thick-walled theory	213.42	213.42	–	–	197.98	197.98	–
	ra_{thick} (%)	82.33	85.70			102.69	88.80	

Table 4
Stress results of the base metal in the pressurizer cylinder (MPa).

Location	Results comparison	External surface of cylinder							
Point ID		T1	T2	T3	T4	T5	T7	Z2	Z4
Longitudinal stress	Test results	99.54	94.04	97.08	103.0	16.69	106.1	104.5	115.7
	Thin-walled theory	105.80	105.80	105.80	105.80	105.80	105.80	105.80	105.80
	ra_{thin} (%)	94.08	88.88	91.76	97.35	15.78	100.28	98.77	109.36
	Thick-walled theory	100.21	100.21	100.21	100.21	100.21	100.21	100.21	100.21
	ra_{thick} (%)	99.33	93.84	96.88	102.78	16.66	105.88	104.28	115.46
Hoop stress	Test results	188.6	183.6	186.6	189.7	47.34	191.8	200.0	200.7
	Thin-walled theory	211.61	211.61	211.61	211.61	211.61	211.61	211.61	211.61
	ra_{thin} (%)	89.13	86.76	88.18	89.65	22.37	90.64	94.51	94.84
	Thick-walled theory	200.43	200.43	200.43	200.43	200.43	200.43	200.43	200.43
	ra_{thick} (%)	94.10	91.60	93.10	94.65	23.62	95.69	99.79	100.13

Table 5
Stress results of the pressurizer upper head (MPa).

Location	Welds at upper head						
Point ID	SR1	SR2	SA1	SA2	SA3	SP1	SP2
σ_1	174.6	130.1	145.6	92.5	167.9	208.4	160.7
σ_2	131.4	86.8	118.3	42.8	106.1	117.0	111.3

Table 6
Stress results of the pressurizer upper head base metal (MPa).

Location Point ID	Results comparison	Welds at upper head T8
σ_1	Test results	170.1
	Theory values	127.23
σ_2	Test results	114.7
	Theory values	127.23

Table 7
Stress results of the pressurizer lower head (MPa).

Location	Surge line nozzle weld	
Point ID	X1	X2
σ_1	143.0	149.7
σ_2	127.8	118.0

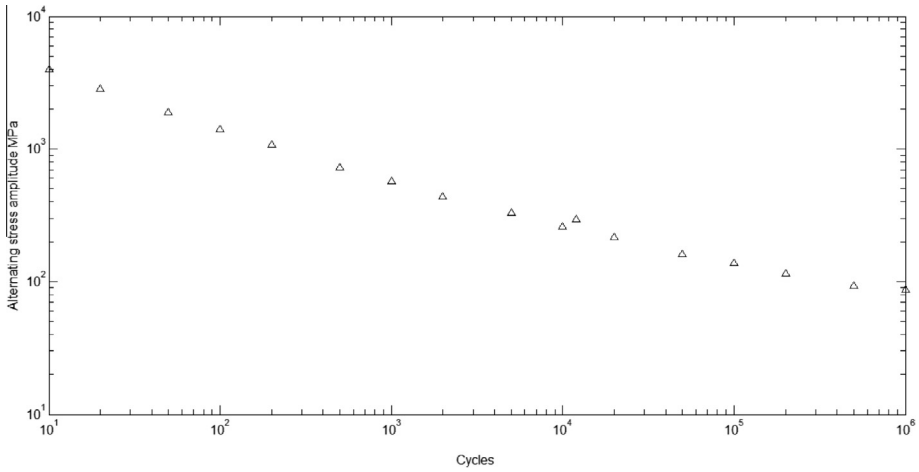

Fig. 10. Fatigue design curve of 16MND5 by the interpolation method.

Stress intensity evaluation

During the hydrostatic test, the final pressure is about 1.5 times the operating pressure, which leads to potential failure risk. According to the RCC-M standard, at testing condition, general primary membrane stress intensity cannot exceed 90% of the yield strength of the material at the test temperature, as described in Eq. (16).

$$P_m \leq 0.9 \times S_y \tag{16}$$

where S_y is the yield strength of material 16MND5 at the test temperature, which is 345 MPa. Therefore, P_m should not exceed 310.5 MPa.

For the cylinder, P_m equals to the hoop stress. For upper head and lower head, P_m equals to the maximum difference among the principal stresses. Thus, according to the stress calculation results, the general primary membrane stress intensity in the outside surface of pressurizer components are as follows,

(1) Longitudinal welds in the cylinder: location Z1 with 203.3 MPa, 65.5% of the allowable value;
(2) Girth welds in the cylinder: location H2 with 182.9 Mpa, 58.9% of the allowable value;
(3) Base metal of cylinder: location Z4 with 200.7 Mpa, 64.6% of the allowable value;
(4) Upper head: location SP1 with 208.4 MPa, 67.1% of the allowable value;
(5) Lower head: location X2 with 149.7 MPa, 48.2% of the allowable value.

The maximum general primary membrane stress in the outside surface of the pressurizer is at point SP1 in upper head spray nozzle weld, and is below the allowable level. According to Eqs. (8) and (13), the general primary membrane stress in the internal surface of the pressurizer can be achieved approximately as follows:

(1) Longitudinal welds in the cylinder: location Z1 with 227.6 MPa, 73.3% of the allowable value;
(2) Girth welds in the cylinder: location H2 with 203.1 MPa, 65.4% of the allowable value;
(3) Base metal of the cylinder: location Z4 with 224.7 MPa, 72.4% of the allowable value;
(4) Upper head: location SP1 with 250.5 MPa, 80.67% of the allowable value;
(5) Lower head: location X2 with 180.1 MPa, 58% of the allowable value.

So the maximum general primary membrane stress in the internal surface of the pressurizer is below the allowable level too.

Fatigue usage factor evaluation

The hydrostatic test includes one cycle of pressure increase and relief, which contributes to the total fatigue usage factor. The fatigue usage factor of one hydrostatic test can be described as Eq. (17),

$$U_i = 1/N_A \tag{17}$$

The fatigue design curve for 16MND5 is achieved by the interpolation method, as shown in Fig. 10. The alternating stress amplitude is calculated according to RCC-M B3232.6. The maximum alternating stress amplitude is calculated as 104.12 MPa at point SP1, which is located at the weld between spry line and upper head, near manhole. From Fig. 10, the

allowable cycle number for alternating stress amplitude of 104.12 MPa is 6.91×10^5, so the attribution of the hydrostatic test to total fatigue life is calculated as follows,

$$U_1 = 1/6.91 \times 10^5 = 1.45 \times 10^{-6} << 1$$

Therefore, one single hydrostatic test has very little effect on the total fatigue life of the pressurizer.

Conclusions

In this paper, actual strain of a CPR1000 unit's pressurizer during the pre-delivery hydrostatic test is acquired. The strain and stress data acquired can be used as the basic data for the pressurizer ageing condition assessment or structural integrity assessment during its long-term operation. The conclusions of this study are summarized as below:

(1) The longitudinal and hoop strains of base metal in the cylinder are very uniform, and the stress values match well with the thick-walled theoretical values. However, the strains of girth and longitudinal welds vary with location. The strains decrease from lower head to upper head, and have the same trend with the circumference deformation variation.
(2) The longitudinal and hoop stresses near the centerline of cylinder middle longitudinal weld are much lower than the stresses at other locations. This indicates the possibility of compressive residual stresses at both longitudinal and circumferential directions.
(3) The principal stresses of symmetrical locations in upper head welds vary a lot. There is possibility that the weld thickness is not uniform along the weld circumference. Also, residual stresses may have contribution to this phenomenon. The principal stresses of symmetrical locations in the surge line nozzle weld agree well. It indicates a good geometric uniformity of this weld.
(4) The maximum general primary membrane stress is at the spray nozzle weld in upper head. The stress value is lower than the allowable value. So the structural integrity is maintained at the highest hydrostatic test pressure. The fatigue usage factor is far less than one, which indicates that a single hydrostatic test cycle has little effect on the total pressurizer fatigue life.

Acknowledgments

The financial support from major state S&T special projects of China (2011ZX06004-002) is greatly acknowledged.

References

[1] Liu Hongwen. Material mechanics. Bei Jing: Higher Education Press; 1992.
[2] Timoshenko SP, Goodier JN. Theory of elasticity. New York: McGraw-Hill; 1970.
[3] Davidson TE, Kendall DP. In: Pugh HLID, editor. The mechanical behavior of materials under pressure. Amsterdam: Elsevier; 1970.
[4] Zhu Ruilin, Li Xiaolin, Wang Chuanshen. Stress and deformation compatibility analysis for thick-walled cylinder. Chem Equip Technol 2008;29(3):61–5.
[5] da Costa Mattos HS, Paim LM, Reis JML. Analysis of burst tests and long-term hydrostatic tests in produced water pipelines. Eng Fail Anal 2012;22:128–40.
[6] Han JY, Jung HY, Cho JR, Choi JH, Bae WB. Buckling analysis and test of composite shells under hydrostatic pressure. J Mater Process Technol 2008;201(1–3):742–5.
[7] Xu James J, Sun Benedict C, Koplic Bermard. Local pressure stresses on lateral pipe-nozzle with various angles of intersection. Nucl Eng Des 2000;199(3):335–40.
[8] Ha JL, Sun BC, Koplic B. Local stress factors of a pipe-nozzle under internal pressure. Nucl Eng Des 1995;157(1–2):81–91.
[9] Schindler S, Zeman JL. Stress concentration factors of nozzle-sphere connections. Int J Press Vessels Pip 2003;80(2):87–95.
[10] Petrovic Aleksandar. Stress analysis in cylindrical pressure vessels with loads applied to the free end of a nozzle. Int J Press Vessels Pip 2001;78(7):485–93.
[11] Rao BSC, Madeswaran R, Chandramohan R. In-fabrication and pre-service care on stainless steel pressure vessels. Int J Press Vessels Pip 1997;73(1):53–7.
[12] Bhuyan GS, Akhtar A, Webster CTL. Effect of hydrostatic retest on the fatigue behaviour of a steel gas cylinder. Pressure Vessel Technol 1991:556–9 (Trans. ASME)113, 4.
[13] Verijenko Victor E, Sarp Adali, Tabakov Pavel Y. Stress distribution in continuously heterogeneous thick laminated pressure vessels. Compos Struct 2001;54(2–3):371–7.
[14] Panagiotopoulos GD. Stress and stability analysis of toroidal shells. Int J Press Vessels Pip 1985;20(2):87–100.
[15] Al-Gahtani H et al. Local pressure testing of spherical vessels. Int J Press Vessels Pip 2014;114–115:61–8.
[16] Kuroda M. A phenomenological plasticity model accounting for hydrostatic stress-sensitivity and vertex-type of effect. Mech Mater 2004;36(3):285–97.
[17] Zingoni Alphose. Stress analysis of a storage vessel in the form of a complete triaxial ellipsoid: hydrostatic effects. Int J Press Vessels Pip 1995;62(3):269–79.
[18] Skopinsky VN. Numerical stress analysis of intersecting cylindrical shells. J Press Ves Technol 1993;115(3):417–24.
[19] Lee Song-In, Koh Seung-Kee. Residual stress effects on the fatigue life of an externally grooved thick-walled pressure vessel. Int J Press Vessels Pip 2002;79:119–26.
[20] French association for design, construction and in-service inspection rules for nuclear island component. Design and construction rules for mechanical components of PWR nuclear islands: RCC-M 2000 + 2002 supplementary. Scientific and Technological Literature Publishing House; 2010. p. 11–31.
[21] The American Society of Mechanical Engineers. Rules for construction of pressure vessels. VIII Division 2, Mandatory Appendix 4-321. New York.: The American Society of Mechanical Engineers; 2004.